



OPEN

Fluorescence quenching based detection of nitroaromatics using luminescent triphenylamine carboxylic acids

Aamnayee Mishra¹, R. Dheepika¹, P. A. Parvathy¹, P. M. Imran², N. S. P. Bhuvanesh³ & S. Nagarajan¹✉

Detection of nitroaromatics employing greener techniques has been one of the most active research fields in chemistry. A series of triphenylamine (TPA) functionalized carboxylic acids were synthesized and characterized using various spectroscopic techniques including single-crystal X-ray diffraction analysis. The interaction of carboxylic acid-decorated TPAs with nitroaromatic compounds was photophysically explored using absorption and emission spectroscopy. Stern–Volmer plot accounts for the appreciable quenching constant of the TPA-acids. Density functional theory calculations were carried out to study the new compounds' frontier molecular orbital energy levels and the possible interactions with picrate anion and revealed an unusual charge transfer interaction between acids and picrate anion. The contact mode detection shows the TPA-acids can be used as dip-strip sensors for picric acid detection.

The easy detection of the toxic and very harmful nitroaromatics for health, environmental and national security reasons has been studied widely by scientists in the last few decades^{1–3}. Nitroaromatic compounds (NAC) are potent explosives and also used in various industries such as pharmaceuticals, dye, and other chemical laboratories^{4,5}, often cause fatal injuries all around the Globe. Many of the NAC are recognized to be mutagenic or carcinogenic⁶. Hence, detecting NAC with high sensitivity is exceedingly anticipated for health, environmental, and security reasons^{7–9}. In earlier days, detecting these hazardous materials involved sophisticated methods^{10–14} and instruments such as GC, HPLC, polarography that are not suitable for real-time applications. Therefore, researchers have been diverted to develop uncomplicated new analytical methods to detect NAC economically in the last two decades^{15–17}.

The technique of fluorescence sensing is a selective, sensitive and convenient method to detect various metals or harmful chemicals. Hence much attention has been drawn to designing and synthesizing efficient small organic fluorophores for the detection of nitroaromatics like picric acid (PA)^{15,18–20}. Several organic fluorophores have been investigated to detect NAC by fluorescence quenching. Various electron-rich molecules like benzo[k]fluoranthene²¹, anthracene-functionalized tris-imidazolium salt²² have been reported to sense PA selectively. In addition, vapor-phase detection of PA has been successfully acquired with PFMI-NP a conjugated polymer nanoparticle²³. Recently tertiary amine-functionalized imidazole-based boron complexes have been reported for selective detection of PA²⁴. Solid-state sensing also provides promising results on the high vapor pressure of nitrobenzene leading to a decrease in fluorescence quenching²⁵. It also showcases the use of paper strips for contact mode detection of PA.

Triphenylamine (TPA) is a suitable class of fluorophores widely used because of their unique geometry and electron-donating property, which provides a suitable optical platform to be modulated for detecting various metal ions as well as harmful compounds^{18,20,26}. TPA has always been used as a crucial molecule taking part in ICT²⁷ making it the widely used molecule for optoelectronic applications^{28,29}. Palas et al.³⁰ reported that strong donor ability of the molecule with extensive π -delocalization may lead to better interaction between electron-deficient PA and the molecule. Duraimurugan et al.²⁰ reported the change in colour of solution due to charge transfer complexation with picrate anion. The work of Chowdhury and Mukherjee on the synthesis of acid groups substituted triarylamines derivatives is worthy to mention here²⁶. They established the existence

¹Department of Chemistry, Central University of Tamil Nadu, Thiruvavur 610 005, India. ²Department of Chemistry, Islamiah College, Vaniyambadi 635 752, India. ³Department of Chemistry, Texas A&M University, College Station, TX 77842, USA. ✉email: snagarajan@cutn.ac.in

of a charge-transfer band which was based on the UV–Vis studies. Solvents such as *N,N*-dimethylformamide (DMF), *N,N*-Dimethylacetamide (DMA), dimethyl sulfoxide (DMSO), PA undergoes deprotonation to form picrate anion, which in turn participated in ground-state charge-transfer complex formation.

Herein we report the design and synthesis of new TPA molecules decorated with the carboxylic acid group(s) for the detection of NACs through fluorescence sensing. Often fluorescent pH probes pertaining to the availability of H⁺ are of greater significance due to various advantages such as non-destructive character, high sensitivity, and specificity^{22,31}. It is essential to design the fluorescent sensors which would easily display fluorescence enhancements, high sensitivity, and selectivity towards the analyte molecule, which inspired us to use the potential –COOH functional groups as they can be easily converted to other activating receptors by forming a PET system^{21,32}. Due to the delocalized π^* excited state, compound's electron density is modulated, which facilitates interaction with electron-deficient nitroaromatic analytes. The interactions are scrutinized by absorption and emission spectroscopic techniques. Multiple fluorescent units amplify the fluorescence quenching through energy and electron transfer and as a result, the interaction studies become efficient. Solution and contact mode detections are also investigated as the cost-effective methodology for NAC detection. This investigation can provide a pathway for selective detection of NAC by the fluorescence quenching method.

Experimental section

Materials. All the materials (triphenylamine, 4-aminobenzonitrile, 4-fluorobenzonitrile, phosphorous(V) oxychloride (POCl₃), potassium permanganate(VII) (KMnO₄), dimethyl sulfoxide (DMSO), potassium hydroxide (KOH), cesium fluoride (CsF), *N,N*-dimethylformamide (DMF), acetone (CH₃COCH₃), ethanol (EtOH)) were used as received from the commercial sources. ACS grade solvents were used without further purification. Column chromatography was carried out with slurry-packed activated silica gel (100–200 mesh). ¹H and ¹³C NMR and was recorded using Bruker 400 MHz instrument in CDCl₃ and d₆ DMSO.

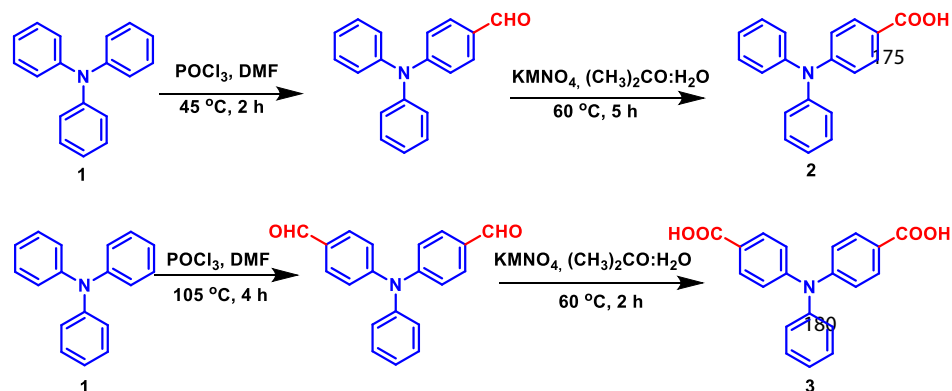
UV–Vis absorption spectra were recorded using a Jasco V-670 spectrophotometer. Perkin Elmer LS 55 spectrofluorimeter was used to obtain the emission spectra. The electrospray ionization mass (ESI–MS) spectra were recorded using THERMO Scientific Exactiveplus UPLC mass spectrometer. Single-crystal x-ray diffraction studies data were collected on a BRUKER APEX2 X-ray (three-circle) diffractometer with Mo- α λ = 0.70173 Å radiation. Microwave-assisted synthesis was performed using a CEM microwave synthesizer. For density functional theory (DFT) studies, the molecules were optimized at the 6–31 D basis level of DFT using Gaussian. The frontier molecular orbital values i.e. highest occupied molecular orbital and lowest unoccupied molecular orbital (HOMO and LUMO) were also extracted.

Synthesis. *General procedure for the synthesis of compounds 2–4.* TPA acids were synthesized as per the reported procedures^{33,34}. In brief, compounds 2 and 3 were synthesized by a two-step synthetic sequence: commercially available triphenylamine (1) was subjected to Vilsmeier Haack formylation followed by oxidation using KMnO₄ in acetone: water (4:1). Compound 4 was prepared by hydrolysis of 4,4',4''-tricyanotriphenylamine using aqueous KOH via microwave-assisted synthesis (Scheme 2).

4-(Diphenylamino)benzoic acid (Compound 2). To a stirred solution of TPA mono aldehyde (1.5 g, 5.49 mmol) in 50 mL acetone–water (4:1), KMnO₄ (4 g, 25.16 mmol) was added portion-wise at 60 °C for 1 h. The reaction was stirred under reflux conditions for 4 h. The acetone was removed under vacuum and water (25 mL) was added and filtered. The filtrate was acidified with HCl to give a white precipitate. The precipitate was filtered and washed with water several times and dried under a vacuum to give compound 2. Pale yellow solid. Yield: 80%. ¹H NMR (400 MHz, d₆ DMSO, δ in ppm): 7.80–7.78 (d, J = 8.0 Hz, 2H); 7.38 (t, J = 7.2 Hz, 4H); 7.17–7.12 (m, 6H); 6.88–6.86 (d, J = 8.4 Hz, 2H); 3.48 (s, 1H). ¹³C NMR (100 MHz, DMSO) δ 167.5, 151.8, 146.5, 131.3, 130.3, 126.2, 125.2, 122.8, 119.4. HRMS (ESI) calculated for C₁₉H₁₅NO₂ [M + H]⁺: 290.1136; found, 290.1183.

4,4'-(Phenylazanediy)l)benzoic acid (Compound 3). 4,4'-Diformyltriphenylamine (0.2 g, 0.66 mmol) was dissolved in a mixture of 15 mL acetone: water (4:1), and the solution was heated. KMnO₄ (0.5 g, 3.3 mmol) was added portion-wise to the mixture for one hour and the reaction mixture was warmed to 60 °C and stirred for 5 h. After removal of acetone, water (10 mL) was added to the residue and the mixture was filtrated and was acidified by slow addition of concentrated HCl. The white precipitate was filtered and dried under a vacuum to afford the product. Crude was recrystallized from DCM and methanol. Yellow small square-shaped crystals formed. Yield: 66%. ¹H NMR (400 MHz, d₆ DMSO, δ in ppm): 12.72 (s, 2H); 7.88–7.86 (d, J = 8.4 Hz, 4H), 7.43 (t, J = 5.9 Hz, 2H); 7.26–7.152 (m, 2H); 7.07–7.05 (d, J = 22.4 Hz, 4H). ¹³C NMR (100 MHz, DMSO) δ 167.2, 150.8, 146.0, 131.4, 130.6, 126.9, 126.0, 125.0, 122.5. HRMS (ESI) calculated for: C₂₀H₁₅NO₄ [M]⁺:333.3374; found: 333.1008.

4,4' 4''-nitrilotribenzoic acid (Compound 4). A mixture of 4-aminobenzonitrile (0.05 g, 0.423 mmol), 4-fluorobenzonitrile (0.11 g, 0.93 mmol), CsF (0.25 g, 1.69 mmol), and 2 mL dry DMF were heated at 140 °C for 20 min under microwave conditions (Power: 155 W, pressure: 250 psi, pre-stirring time: 1 min). Progress of the reaction was monitored by TLC. After the completion, the reaction mixture was poured into ice-cold water. The solid product was filtered and washed with plenty of water. The product was dried under a vacuum. The crude product was dissolved in EtOH: KOH (3:1) and heated at 110 °C for 20 min under microwave conditions (Power: 155 W, pressure: 250 psi, pre-stirring time: 1 min). Completion of the reaction was monitored by TLC. After cooling down to room temperature the mixture was acidified with 3 N HCl to pH 3 to get a white precipitate. Finally, the precipitate was filtered and washed with plenty of water, dried in an oven to obtain the desired product. Pale yellow solid. Yield: 80%. ¹H NMR (400 MHz, d₆ DMSO, δ in ppm): 12.81 (s, 3H); 7.92–7.90 (d,



Scheme 1. Synthesis of compounds 2 and 3.

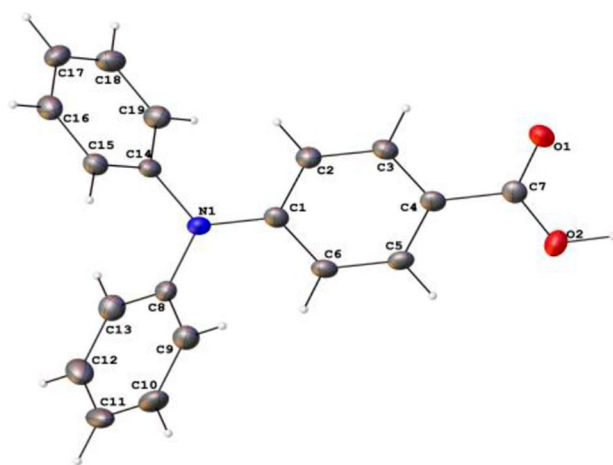


Figure 1. The thermal ellipsoidal plot of compound 2 (TPA monoacid). The unit cell dimensions are $a = 9.1921(6) \text{ \AA}$, $b = 9.6185(7) \text{ \AA}$, $c = 17.1694(11) \text{ \AA}$, $\alpha = 90^\circ$, $\beta = 90.068(2)^\circ$, $\gamma = 90^\circ$. The crystal system is monoclinic with a volume of $1518.02(18) \text{ \AA}^3$.

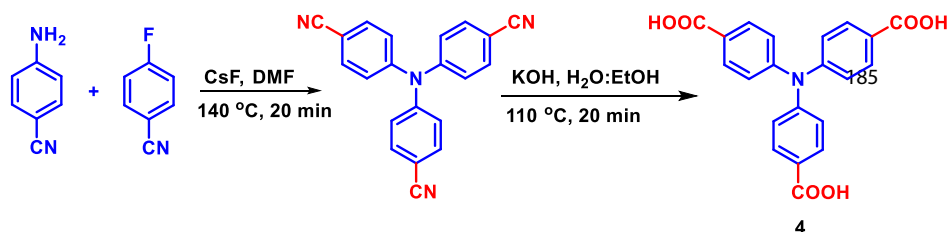
$J = 7.2 \text{ Hz}$, 6H); 7.15–7.13 (d, $J = 7.2 \text{ Hz}$, 6H). ¹³C NMR (100 MHz, DMSO) δ 167.1, 150.2, 131.6, 126.3, 124.1. HRMS (ESI) calculated for: C₂₁H₁₅NO₆ [M-H]⁻: 376.0821; found 376.0828.

Preparation of solutions. Stock solutions (10^{-3} M) were prepared by weighing the calculated amount of the compounds and dissolving in the calculated volume (10 mL) of DMSO solvent. Further dilution was made for desired concentration for photophysical studies. Similarly, the stock solutions (10^{-3} M) of NAC were made by dissolving the calculated amount of appropriate compound in DMSO solvent. Solutions were diluted further for photophysical studies.

Photophysical studies. For UV–Vis absorption, the TPA compounds at 10^{-5} M concentration were titrated against nitroaromatics (10^{-4} M), and the corresponding responses were recorded. 100 μL of particular NAC was successively added to 2 mL of the compound for photophysical studies. For Fluorescence titration, dilute solutions of the compounds 1–4 (10^{-7} M) were titrated with nitroaromatics (10^{-5} M), particularly for PA response was recorded for the compounds 1–4 in 10^{-6} M .

Results and discussions

TPA can be used as a three-armed fluorescent probe³⁵, due to its high fluorescent nature and solubility in a wide range of solvents. The substitution will alter its photophysical properties. Recent reports suggest that TPA molecules are used as sensors to detect harmful chemicals and biologically important metal ions^{18,20,26,30}. Hence, we designed and synthesized mono, di, and tri TPA carboxylic acids with modulated electron density for sensing applications. In addition, deprotonation of carboxylic acids will also lead to some interesting studies. The synthetic pathway is given in Scheme 1 and 2. Quenching of emission intensity of an electron-rich fluorophore by electron-poor nitroaromatics is associated with an intermolecular photoinduced donor–acceptor electron transfer mechanism. All the synthesized compounds are well characterized by NMR, spectroscopic techniques including single-crystal XRD (Fig. 1).



Scheme 2. Microwave-assisted synthesis of compound 4.

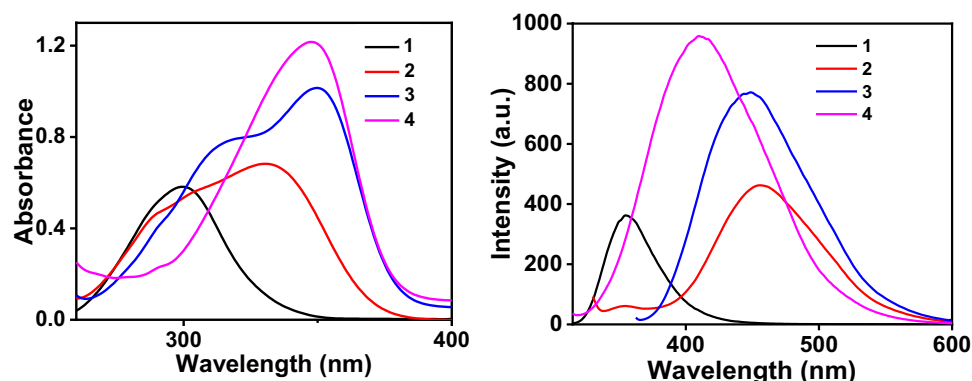


Figure 2. (a) UV-Vis absorption and (b) emission spectra of compounds 1–4.

C. no	λ_{Abs} (nm)	λ_{Em} (nm)	Stokes' shift (nm)	Absorption co-efficient (ϵ , $10^4 \text{ L mol}^{-1} \text{ cm}^{-1}$)
1	300	355.5	55.5	5.8
2	331	457.8	126.8	6.8
3	350	445.9	95.9	10.1
4	348	412.0	64.0	12.1

Table 1. Photophysical properties of compounds 1–4.

Optical properties. The absorption spectra of the compounds 1–4 in DMSO show a single absorption peak in the range of 300–348 nm, corresponding to π - π^* transition of the conjugated TPA core. For compound 3 in addition, a shoulder peak is also obtained at 317 nm which might be due to the intramolecular charge transfer (ICT).

The absorption and emission spectra are shown in Fig. 2a,b, respectively. When the medium is polar high charge separation leads to a change in dipole moment and instigates the molecule to attain a different geometry in the excited state. The excited state transitions involved (in vibrational levels of S_1 and S_0) are different than that of the absorption in the case of compounds 2 and 3 (TPA monoacid and di acid respectively) resulting in the breakdown of mirror-image symmetry^{36–38}.

The area under the peak is increasing with the increase of the number of carboxylic acid groups, concluding the fact that an increase in the number of acid groups increases fluorescence intensity, binding capacity thereby using the effect of the autochrome -COOH. Compound 2 shows the most significant Stokes' shift of 126.8 nm indicating a large change in the dipole moment of the molecule after excitation relevant to Table 1 confirming its value to be 7.15D. Polar solvent DMSO activates the probable intermolecular charge transfer from one part (donor) of the molecule to the other (acceptor) in the excited state. While 4 (TPA tri acid) shows the least value of 64.0 nm among the three acids as well as compound 4 (TPA tri acid) has the highest absorption coefficient of $12.1 \times 10^4 \text{ L mol}^{-1} \text{ cm}^{-1}$ making it an interesting molecule for fluorescence studies.

Interaction with nitroaromatics. To get an insight into the interaction of compounds, 1–4 with electron-deficient nitroaromatics such as 2,4,6-trinitrophenol (PA), 4-nitroaniline, 4-nitrotoluene, 4-nitrobenzoic acid, 4-nitrobenzaldehyde, and 2-nitrophenol absorption and emission studies were carried out. The studied NACs in our case caused quenching of fluorescence, out of which PA shows better quenching. In the case of PA, the colour change is observed for the naked eye. In compound 4, the quenching was two-fold with PA might be due to the increased number of acid groups. In addition, this two-fold quenching may be due to excited state

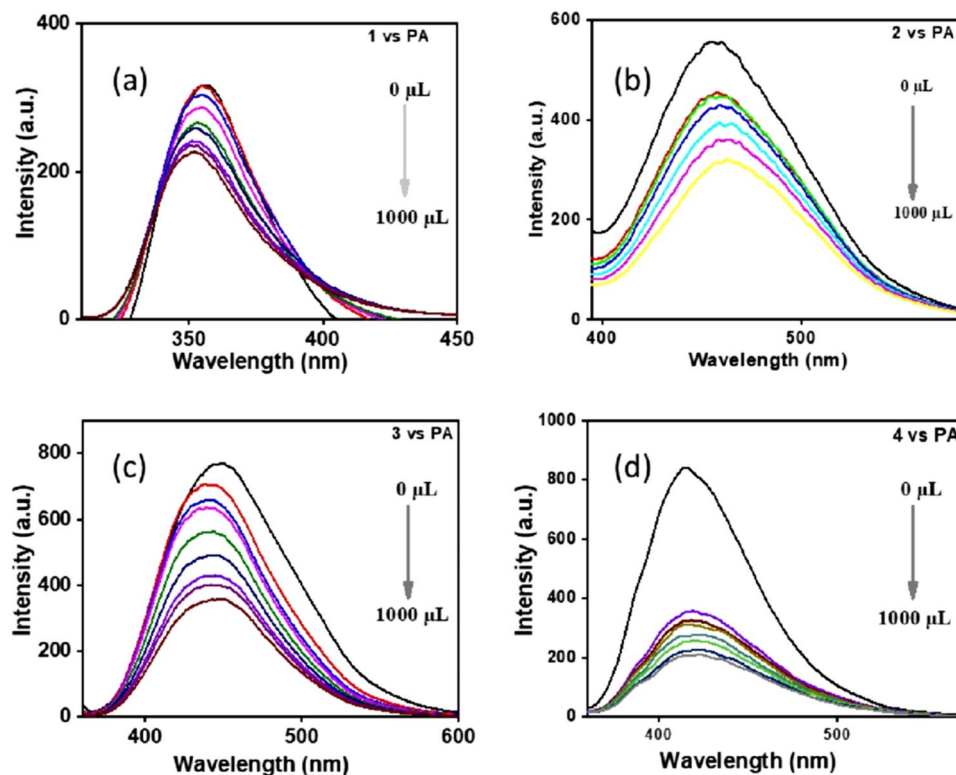


Figure 3. Fluorescence spectra of compounds 1–4 in the presence of picric acid (PA). The concentration of picric acid in DMSO is in the order of 0 M, 4.76×10^{-6} M, 9.09×10^{-6} M, 13.0×10^{-6} M, 20.0×10^{-6} M, 25.9×10^{-6} M, 31.0×10^{-6} M and 33.3×10^{-6} M for all (additions of 0 μ L, 100 μ L, 200 μ L, 300 μ L, 500 μ L, 700 μ L, 900 μ L, and 1000 μ L).

electron transfer between the twisted structure of the fluorophore and picric acid. Similarly, the interaction of 4-nitrotoluene with **2** dramatically decreases the fluorescence intensity of the sensor, leading to an exciting result of a twofold quenching of fluorescence and high sensitivity of the sensor TPA di acid (**2**) towards the harmful nitrotoluene³⁶. The results are shown in Figs. 3 and 4. All the other interactions are given in supplementary data (Supplementary data)

The high quenching efficiency of PA can be attributed to deprotonation of strongly acidic phenolic –OH group followed by anion exchange with the sensor molecule²². In the case of conventional fluorophores³⁹ featured with π -planar structures usually suffer from serious self-quenching in the aggregated state, poor photostability, and small Stokes' shift values. In DMSO, PA undergoes deprotonation to form a picric anion, which takes part in the ground state charge transfer complex formation. Thus, polar solvent like DMSO enhances the binding affinity of analyte and sensor. To gain an insight into the quenching efficiency, the Stern–Volmer quenching constant was calculated by the equation ($I_0/I = 1 + K_{SV} [Q]$). Where I_0 and I are the fluorescence intensity before and after the addition of PA, $[Q]$ is the concentration of PA. The linearity of the plots supports the static quenching mechanism by a ground state charge transfer between the analytes and sensors²⁰ (Fig. 5) Among the three compounds studied, **4** has shown better results with a high K_{SV} quenching constant value of $9.715 \times 10^5 \text{ M}^{-1}$ due to the number of the acid groups increased indicating that the TPA tri acid molecule exhibited better binding interactions with the analyte. It also reveals that the TPA tri acid is the best candidate for working as a fluorescent sensor owing to its sensitivity^{36,40}.

Whereas **1** and **3** showed relatively lower quenching constant values of $1.074 \times 10^5 \text{ M}^{-1}$ and $1.908 \times 10^5 \text{ M}^{-1}$ respectively (Fig. 5) contributing to the idea of excited state twisted geometry leading to poor binding interactions. Micro molar level of detection was achieved with our molecules under study as pertinent with other fluorophores³⁸ The reported molecules showed high Stokes' shift as well as good quenching efficiency for nitroaromatics by overcoming the aforementioned issues such as self-quenching in the aggregated state and poor photostability.

The response towards other NACs. Along with PA and 4-nitrotoluene, several other nitro compounds such as 4-nitroaniline, 4-nitrobenzoic acid, 4-nitrobenzaldehyde, and 2-nitrophenol were used to check the selectivity of the sensors. The quenching of the emission intensity in other NACs was found to be insignificant as compared to the cases with PA and 4-nitrotoluene.

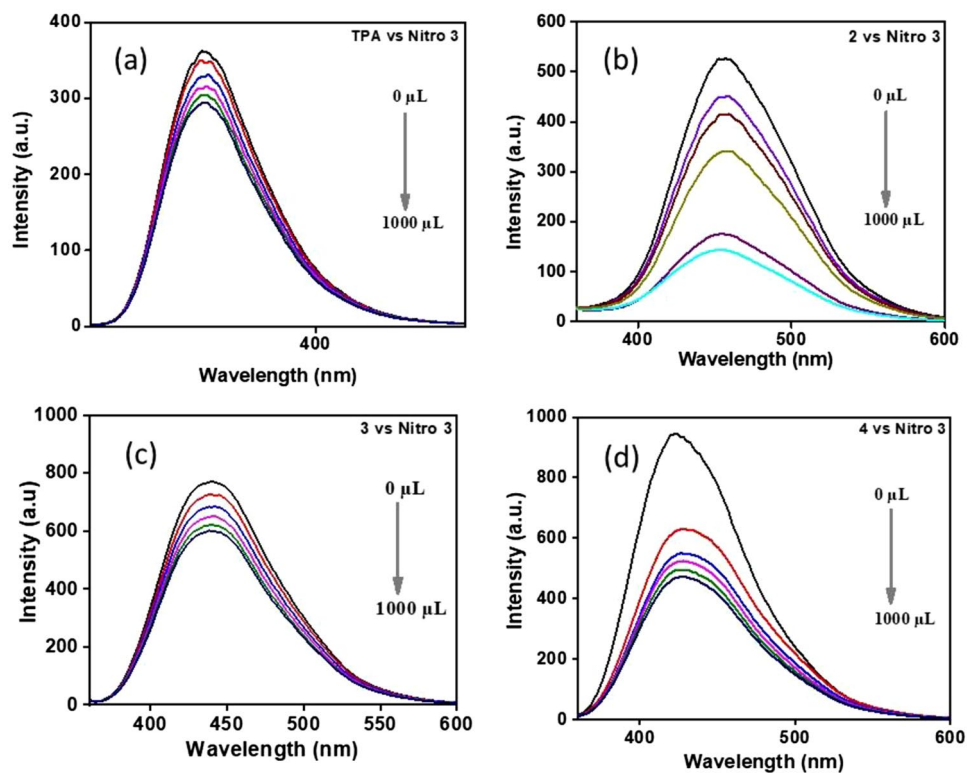


Figure 4. Fluorescence spectra of compounds 1–4 in the presence of 4-Nitrotoluene (Nitro 3). The concentration of 4-Nitrotoluene in DMSO is in the order of 0 M, 9.09×10^{-5} M, 16.6×10^{-5} M, 23.0×10^{-5} M, 28.5×10^{-5} M, and 33.3×10^{-5} M for all (additions of 0 μL , 200 μL , 400 μL , 600 μL , 800 μL , and 1000 μL).

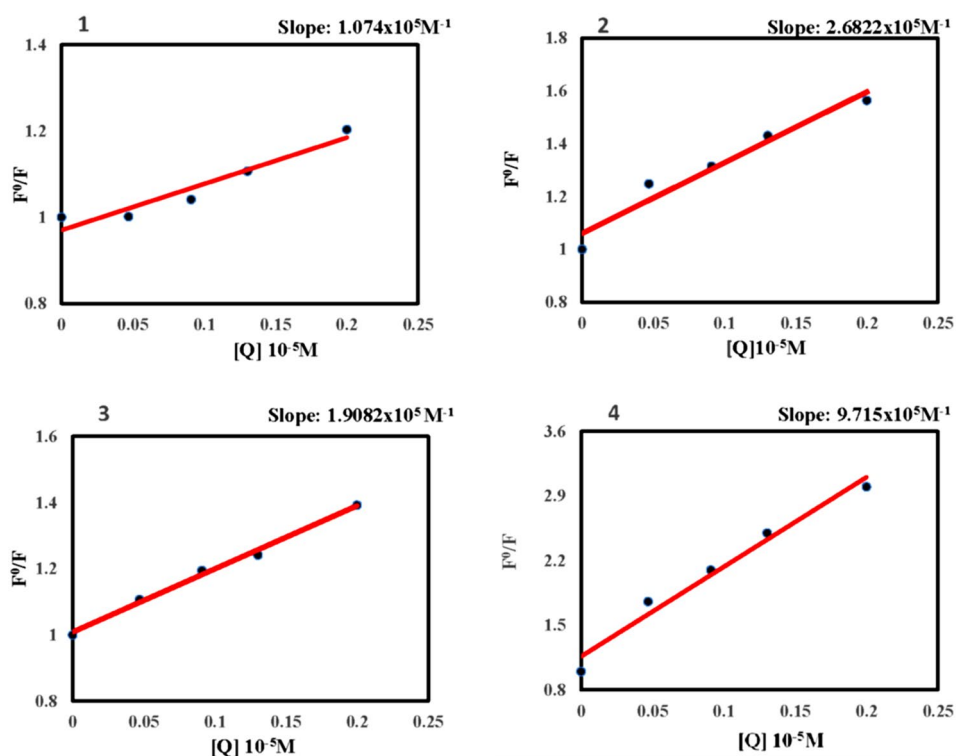


Figure 5. Stern–Volmer plots of compounds 1–4.

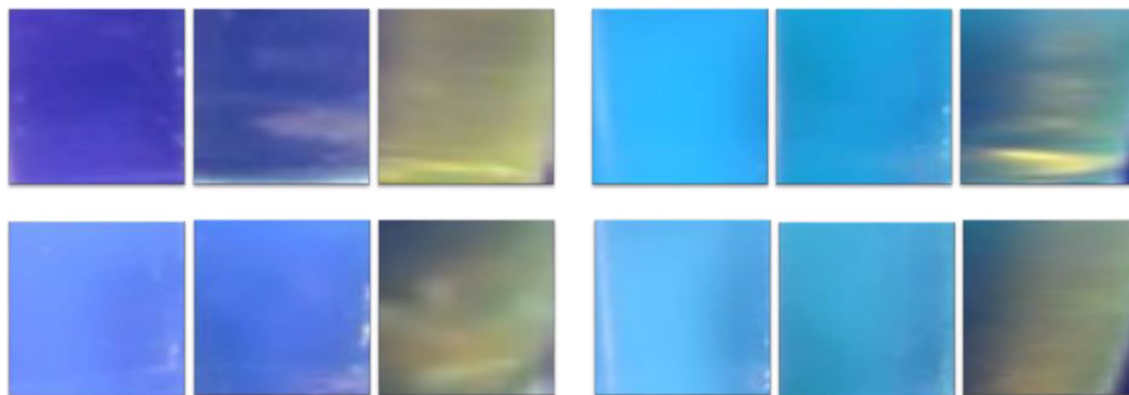


Figure 6. Visual color change (under UV light) upon gradual addition of 10^{-4} M PA to 4 mL of 10^{-6} M solution of compounds **1**, **2**, **3** and **4** in DMSO, (left, 0 μ L; middle: 50 μ L; right: 300 μ L).

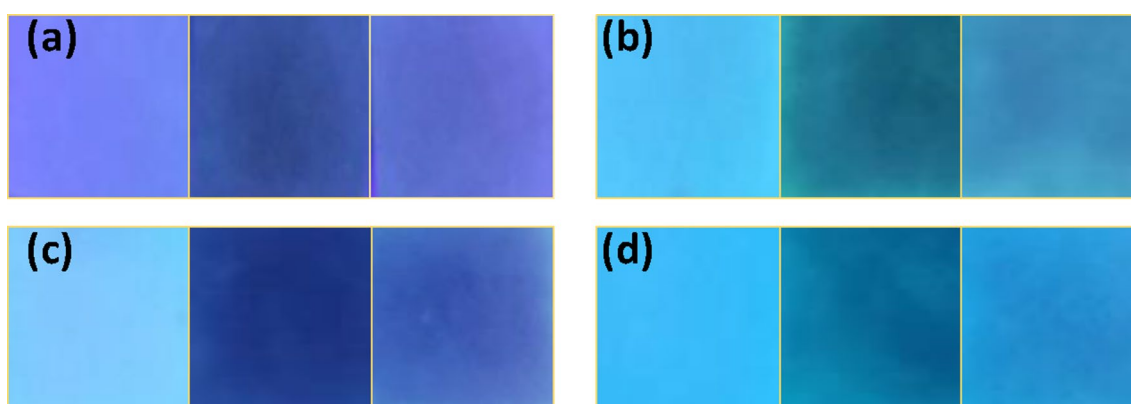


Figure 7. Paper strip images of compounds **1–4** after the addition of different concentrations of PA. (0 M, 10^{-3} M, 10^{-11} M).

Solution mode detection. Visual detection of harmful nitroaromatic compounds is important for personal safety and environmental reasons, and low cost-high efficiency is an added benefit^{39,41,42}. For visual detection, 10^{-4} M PA was slowly added to 10^{-6} M solutions of compounds **1**, **2**, **3**, and **4** incrementally as shown in Fig. 6. On subsequent addition of PA, the fluorescence quenched from blue to non-fluorescent, which is consistent with the previously obtained result²⁶.

Contact mode detection. For contact-mode detection, Whatman 42 filter paper was cut into 2 cm² pieces and dipped into the concentrated solutions of the compounds **1–4** for 10 min and dried subsequently under reduced pressure. After complete drying, the strips were introduced to different concentration solutions of PA (from 10^{-3} to 10^{-11} M). 10 μ L of PA was drop-casted onto the freshly prepared test strips. The test strips were then analyzed under a UV lamp and given in Fig. 7. Dark spots were obtained for concentrated PA. The colour of the spot faded upon decreasing the concentration.

Computational studies. To get an idea about the electronic distribution in the frontier orbitals of compounds, density functional theory (DFT) calculations were carried out. The molecules were optimized at the 6–31 D basis level of DFT using Gaussian and shown in Fig. 8. Frontier molecular orbital values (HOMO and LUMO) are given in Fig. 9 and the HOMO–LUMO energy levels of Compounds **1–4** are given in Table 2. The fluorescence quenching mechanism can be explained by donor–acceptor charge transfer between picrate anion and sensor molecule. Charge transfer is the probable way of quenching fluorescence as the HOMO of compounds **1–4** is situated near the LUMO of the picrate. The LUMO of picrate anion (4.5 eV) is situated near the HOMO of fluorophores (5.7 eV). The feasible mechanism of fluorescence quenching stipulates the idea of a ground state charge transfer from sensor molecules to the electron-deficient PA which was also evident from the DFT calculation²².

Conclusion

In summary, we have developed a set of carboxylic acid group decorated triphenylamines (**2–4**) for the efficient detection of nitroaromatics. The molecules showed appreciable quenching in fluorescence by nitroaromatics. Our molecules showed high Stokes' shift (126.8 nm for compound **2**) as well as good quenching efficiency.

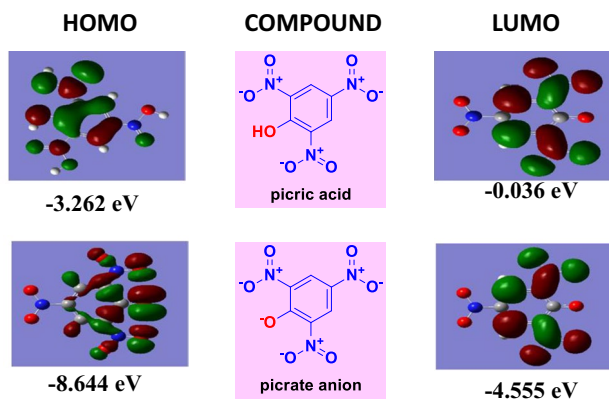


Figure 8. HOMO–LUMO of picric acid and picrate anion.

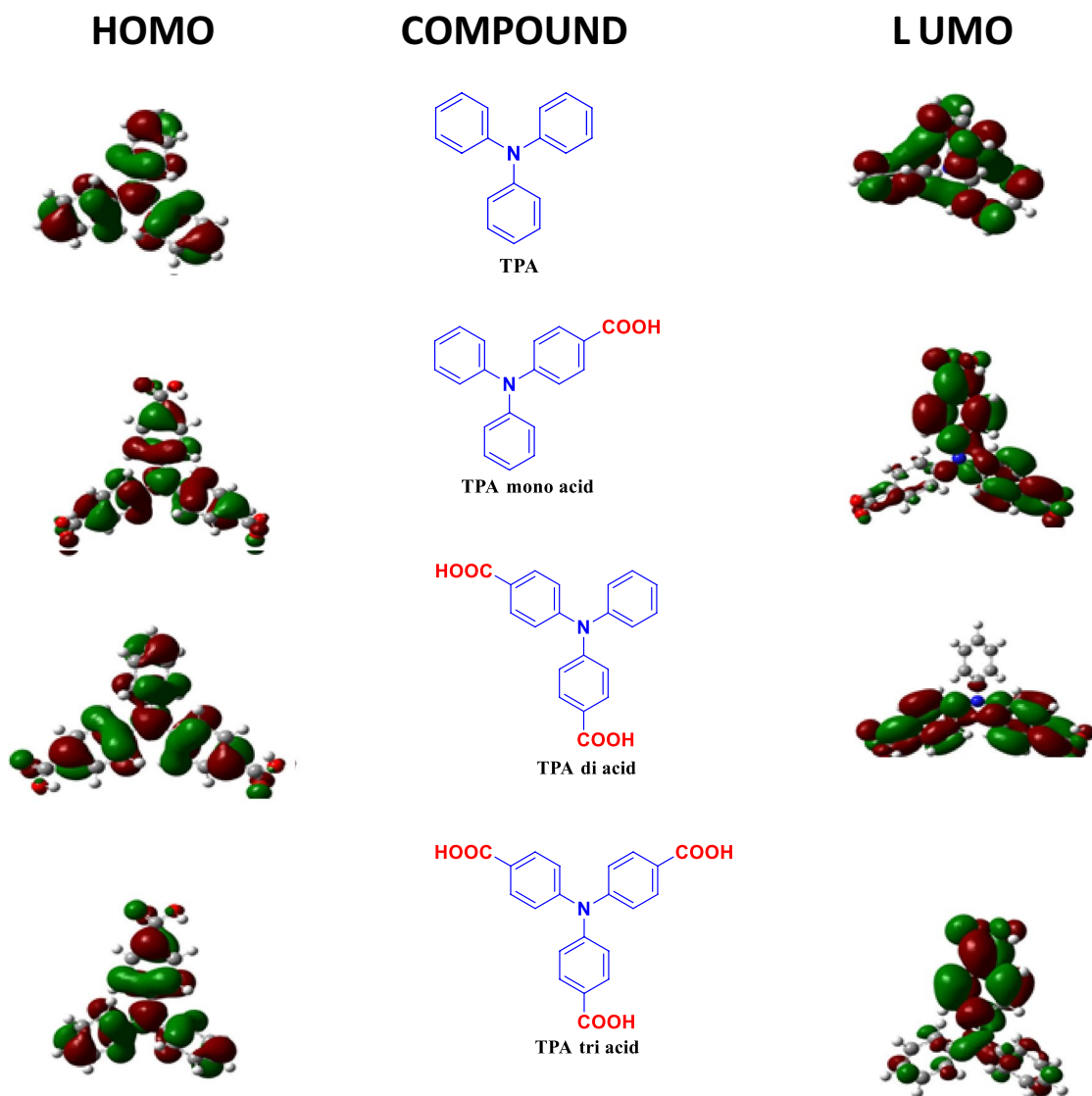


Figure 9. HOMO–LUMO of compounds 1–4.

Compound	Molecular formula	DFT energy (Hartree)	HOMO (eV)	LUMO (eV)	Band gap (eV)	Dipole D
1	C ₁₈ H ₁₅ IN	-749.524	-5.2420	-0.8172	4.42487	0.0067
2	C ₁₉ H ₁₅ NO ₂	-938.020	-5.7142	-1.6833	4.03085	6.8238
3	C ₂₀ H ₁₅ NO ₄	-1126.51	-6.1057	-2.1913	3.91438	7.1509
4	C ₂₁ H ₁₅ NO ₆	-1315.43	-6.4434	-2.4504	3.99303	2.9945

Table 2. Listing the HOMO–LUMO energy levels of Compounds 1–4.

From photophysical studies, it is evident that compounds 2–4 underwent concentration-dependent fluorescence quenching by π - π interaction. Solution state fluorescence titration study revealed that all of the compounds have a high binding affinity (quenching constant value of compound 4 is $9.715 \times 10^5 \text{ M}^{-1}$) for picrate anion. The quenching of fluorescence may be due to the sensor to picrate charge transfer in ground-state complex formation as well as resonance energy transfer between picrate and sensor molecules. DFT calculations gave an insight into the energy levels of the molecules and PA. From the contact mode, it was concluded that these acids can be used as dip-strip sensors for picric acid cost-effectively.

Received: 26 June 2021; Accepted: 26 August 2021

Published online: 29 September 2021

References

- Chen, Y., Lam, J. W. Y., Kwok, R. T. K., Liu, B. & Tang, B. Z. Aggregation-induced emission: Fundamental understanding and future developments. *Mater. Horiz.* **6**(3), 428–433 (2019).
- Albert, K. J. *et al.* Cross-reactive chemical sensor arrays. *Chem. Rev.* **100**(7), 2595–2626. <https://doi.org/10.1021/cr980102w> (2000).
- Zyryanov, G. V. *et al.* Chemosensors for detection of nitroaromatic compounds (explosives). *Russ. Chem. Rev.* **83**(9), 783. <https://doi.org/10.1070/RC2014v083n09ABEH004467> (2014).
- Ju, K.-S. & Parales, R. E. Nitroaromatic compounds, from synthesis to biodegradation. *Microbiol. Mol. Biol. Rev.* **74**(2), 250–272. <https://doi.org/10.1128/MMBR.00006-10> (2010).
- Olender, D., Zwawiak, J. & Zaprutko, L. Multidirectional efficacy of biologically active nitro compounds included in medicines. *Pharm. Basel Switz.* <https://doi.org/10.3390/ph11020054> (2018).
- Tokawa, H., Nakagawa, R., Horikawa, K. & Ohkubo, A. The nature of the mutagenicity and carcinogenicity of nitrated, aromatic compounds in the environment. *Environ. Health Perspect.* **73**, 191–199. <https://doi.org/10.1289/ehp.8773191> (1987).
- Ma, R.-M., Ota, S., Li, Y., Yang, S. & Zhang, X. Explosives detection in a lasing plasmon nanocavity. *Nat. Nanotechnol.* **9**(8), 600–604. <https://doi.org/10.1038/nnano.2014.135> (2014).
- Shanmugaraju, S. & Mukherjee, P. S. Self-Assembled discrete molecules for sensing nitroaromatics. *Chem. Weinh. Bergstr. Ger.* **21**(18), 6656–6666. <https://doi.org/10.1002/chem.201386092> (2015).
- Hu, Z., Deibert, B. J. & Li, J. Luminescent metal-organic frameworks for chemical sensing and explosive detection. *Chem. Soc. Rev.* **43**(16), 5815–5840. <https://doi.org/10.1039/C4CS00010B> (2014).
- Germain, M. E. & Knapp, M. J. Optical explosives detection: from color changes to fluorescence turn-on. *Chem. Soc. Rev.* **38**(9), 2543–2555. <https://doi.org/10.1039/B809631G> (2009).
- Dasary, S. S. R. *et al.* Highly sensitive and selective dynamic light-scattering assay for TNT detection using p-ATP attached gold nanoparticle. *ACS Appl. Mater. Interfaces* **2**(12), 3455–3460. <https://doi.org/10.1021/am1005139> (2010).
- Enkin, N., Sharon, E., Golub, E. & Willner, I. Ag Nanocluster/DNA hybrids: functional modules for the detection of nitroaromatic and RDX explosives. *Nano Lett.* **14**(8), 4918–4922. <https://doi.org/10.1021/nl502720s> (2014).
- Díaz Aguilar, A. *et al.* A hybrid nanosensor for TNT vapor detection. *Nano Lett.* **10**(2), 380–384. <https://doi.org/10.1021/nl902382s> (2010).
- Czarnik, A. W. A sense for landmines. *Nature* **394**(6692), 417–418. <https://doi.org/10.1038/28728> (1998).
- Sun, X., Wang, Y. & Lei, Y. Fluorescence based explosive detection: from mechanisms to sensory materials. *Chem. Soc. Rev.* **44**(22), 8019–8061. <https://doi.org/10.1039/C5CS00496A> (2015).
- Bailey, C. G. & Yan, C. Separation of explosives using capillary electrochromatography. *Anal. Chem.* **70**(15), 3275–3279. <https://doi.org/10.1021/ac980042u> (1998).
- Sylvia, J. M., Janni, J. A., Klein, J. D. & Spencer, K. M. Surface-enhanced raman detection of 2,4-dinitrotoluene impurity vapor as a marker to locate landmines. *Anal. Chem.* **72**(23), 5834–5840. <https://doi.org/10.1021/ac0006573> (2000).
- Sonalin, S., Pandikassala, A., Dheepika, R., Imran, P. K. M. & Nagarajan, S. Molecular aggregation stimulated tunable emission behaviour of functionalized 1, 8 naphthalimides. *J. Lumin.* **215**, 116699–187167. <https://doi.org/10.1016/j.jlumin.2019.116699> (2019).
- Boobalan, G., Imran, P. M., Ramkumar, S. G. & Nagarajan, S. Fabrication of luminescent perylene bisimide nanorods. *J. Lumin.* **146**, 387–393. <https://doi.org/10.1016/j.jlumin.2013.10.009> (2014).
- Duraimurugan, K., Balasaravanan, R. & Siva, A. Electron rich triphenylamine derivatives (D- π -D) for selective sensing of picric acid in aqueous media. *Sens. Actuators B Chem.* **231**, 302–312. <https://doi.org/10.1016/j.snb.2016.03.035> (2016).
- Patra, D. & Mishra, A. K. Fluorescence quenching of benzo[k]fluoranthene in poly(vinyl alcohol) film: A possible optical sensor for nitro aromatic compounds. *Sens. Actuators B Chem.* **80**(3), 278–282. [https://doi.org/10.1016/S0925-4005\(01\)00919-4](https://doi.org/10.1016/S0925-4005(01)00919-4) (2001).
- Roy, B., Bar, A. K., Gole, B. & Mukherjee, P. S. Fluorescent tris-imidazolium sensors for picric acid explosive. *J. Org. Chem.* **78**(3), 1306–1310. <https://doi.org/10.1021/jo302585a> (2013).
- Malik, A. H., Hussain, S., Kalita, A. & Iyer, P. K. Conjugated polymer nanoparticles for the amplified detection of nitro-explosive picric acid on multiple platforms. *ACS Appl. Mater. Interfaces* **7**(48), 26968–26976. <https://doi.org/10.1021/acsami.5b08068> (2015).
- Dhanunjayarao, K., Mukundam, V. & Venkatasubbaiah, K. Tetracoordinate imidazole-based boron complexes for the selective detection of picric acid. *Inorg. Chem.* **55**(21), 11153–11159. <https://doi.org/10.1021/acs.inorgchem.6b01767> (2016).
- Costa, A. I., Pinto, H. D., Ferreira, L. F. V. & Prata, J. V. Solid-state sensory properties of CALIX-poly(phenylene ethynylene)s toward nitroaromatic explosives. *Sens. Actuators B Chem.* **161**(1), 702–713. <https://doi.org/10.1016/j.snb.2011.11.017> (2012).
- Chowdhury, A. & Mukherjee, P. S. Electron-rich triphenylamine-based sensors for picric acid detection. *J. Org. Chem.* **80**(8), 4064–4075. <https://doi.org/10.1021/acs.joc.5b00348> (2015).
- Dumur, F. & Goubard, F. Triphenylamines and 1,3,4-oxadiazoles: A versatile combination for controlling the charge balance in organic electronics. *New J. Chem.* **38**(6), 2204–2224. <https://doi.org/10.1039/C3NJ01537H> (2014).

28. Zhao, Z. *et al.* Full Emission color tuning in luminogens constructed from tetraphenylethene, benzo-2,1,3-thiadiazole and thiophene building blocks. *Chem. Commun.* **47**(31), 8847–8849. <https://doi.org/10.1039/C1CC12775F> (2011).
29. Li, H. *et al.* New thermally stable aggregation-induced emission enhancement compounds for non-doped red organic light-emitting diodes. *Chem. Commun.* **47**(40), 11273–11275. <https://doi.org/10.1039/C1CC14642D> (2011).
30. Pati, P. B. & Zade, S. S. Highly emissive triphenylamine based fluorophores for detection of picric acid. *Tetrahedron Lett.* **55**(38), 5290–5293. <https://doi.org/10.1016/j.tetlet.2014.07.098> (2014).
31. Zhao, Y. *et al.* Benzimidazo[2,1-a]benz[de]Isoquinoline-7-one-12-carboxylic acid based fluorescent sensors for pH and Fe³⁺. *J. Photochem. Photobiol. A Chem.* **314**, 52–59. <https://doi.org/10.1016/j.jphotochem.2015.08.003> (2016).
32. Liu, Z. *et al.* Novel fluorescent sensors based on benzimidazo [2,1-a]benz[de]Isoquinoline-7-One-12-carboxylic acid for Cu²⁺. *RSC Adv.* **4**(100), 56863–56869. <https://doi.org/10.1039/c4ra12242a> (2014).
33. Ghosh, K. & Saha, I. Triphenylamine-based simple chemosensor for selective fluorometric detection of fluoride, acetate and dihydrogenphosphate ions in different solvents. *J. Incl. Phenom. Macrocycl. Chem.* **70**(1), 97–107. <https://doi.org/10.1007/s10847-010-9866-5> (2011).
34. Nandi, S., Chakraborty, D. & Vaidhyanathan, R. A permanently porous single molecule H-bonded organic framework for selective CO₂ capture. *Chem. Commun.* **52**(45), 7249–7252. <https://doi.org/10.1039/C6CC02964G> (2016).
35. Mei, J., Leung, N. L. C., Kwok, R. T. K., Lam, J. W. Y. & Tang, B. Z. Aggregation-induced emission: Together we shine, united we soar!. *Chem. Rev.* **115**(21), 11718–11940. <https://doi.org/10.1021/acs.chemrev.5b00263> (2015).
36. Yan, J. *et al.* The nitro aromatic compounds detection by triazole carboxylic acid and its complex with the fluorescent property. *Tetrahedron* **73**(18), 2682–2689. <https://doi.org/10.1016/j.tet.2017.03.057> (2017).
37. Heimel, G. *et al.* Breakdown of the mirror image symmetry in the optical absorption/emission spectra of oligo(para-phenylene) s. *J. Chem. Phys.* **122**, 054501. <https://doi.org/10.1063/1.1839574> (2005).
38. Nath, S. *et al.* A Sensitive and selective sensor for picric acid detection with a fluorescence switching response. *New J. Chem.* **42**(7), 5382–5394. <https://doi.org/10.1039/c7nj05136k> (2018).
39. Peng, Y., Zhang, A.-J., Dong, M. & Wang, Y.-W. A colorimetric and fluorescent chemosensor for the detection of an explosive—2,4,6-trinitrophenol (TNP). *Chem. Commun.* **47**(15), 4505–4507. <https://doi.org/10.1039/C1CC10400D> (2011).
40. Mako, T. L., Racicot, J. M. & Levine, M. Supramolecular luminescent sensors. *Chem. Rev.* **119**(1), 322–477. <https://doi.org/10.1021/acs.chemrev.8b00260> (2019).
41. Sohn, H., Calhoun, R. M., Sailor, M. J. & Trogler, W. C. Detection of TNT and picric acid on surfaces and in seawater by using photoluminescent polysiloles. *Angew. Chem. Int. Ed.* **2001**, **40**(11), 2104–2105. [https://doi.org/10.1002/1521-3773\(20010601\)40:11<2104::AID-ANIE2104>3.0.CO;2](https://doi.org/10.1002/1521-3773(20010601)40:11<2104::AID-ANIE2104>3.0.CO;2).
42. Lee, J. H., Kang, S., Lee, J. Y., Jaworski, J. & Jung, J. H. Instant visual detection of picogram levels of trinitrotoluene by using luminescent metal-organic framework gel-coated filter paper. *Chem. Eur. J.* **19**(49), 16665–16671. <https://doi.org/10.1002/chem.201301507> (2013).

Acknowledgements

The authors are thankful to the Central University of Tamil Nadu, India for the facilities provided.

Author contributions

A.M.: Synthesis, Formal Analysis, Methodology, Writing—original draft. R.D.: Validation, Writing edit P.A.P.: Synthesis and analysis. P.M.I.: Computational studies N.S.P.B. Single Crystal. S.N. Conceptualization, Supervision, Project administration.

Competing interests

The authors declare no competing interests.

Additional information

Supplementary Information The online version contains supplementary material available at <https://doi.org/10.1038/s41598-021-97832-0>.

Correspondence and requests for materials should be addressed to S.N.

Reprints and permissions information is available at www.nature.com/reprints.

Publisher's note Springer Nature remains neutral with regard to jurisdictional claims in published maps and institutional affiliations.



Open Access This article is licensed under a Creative Commons Attribution 4.0 International License, which permits use, sharing, adaptation, distribution and reproduction in any medium or format, as long as you give appropriate credit to the original author(s) and the source, provide a link to the Creative Commons licence, and indicate if changes were made. The images or other third party material in this article are included in the article's Creative Commons licence, unless indicated otherwise in a credit line to the material. If material is not included in the article's Creative Commons licence and your intended use is not permitted by statutory regulation or exceeds the permitted use, you will need to obtain permission directly from the copyright holder. To view a copy of this licence, visit <http://creativecommons.org/licenses/by/4.0/>.

© The Author(s) 2021